

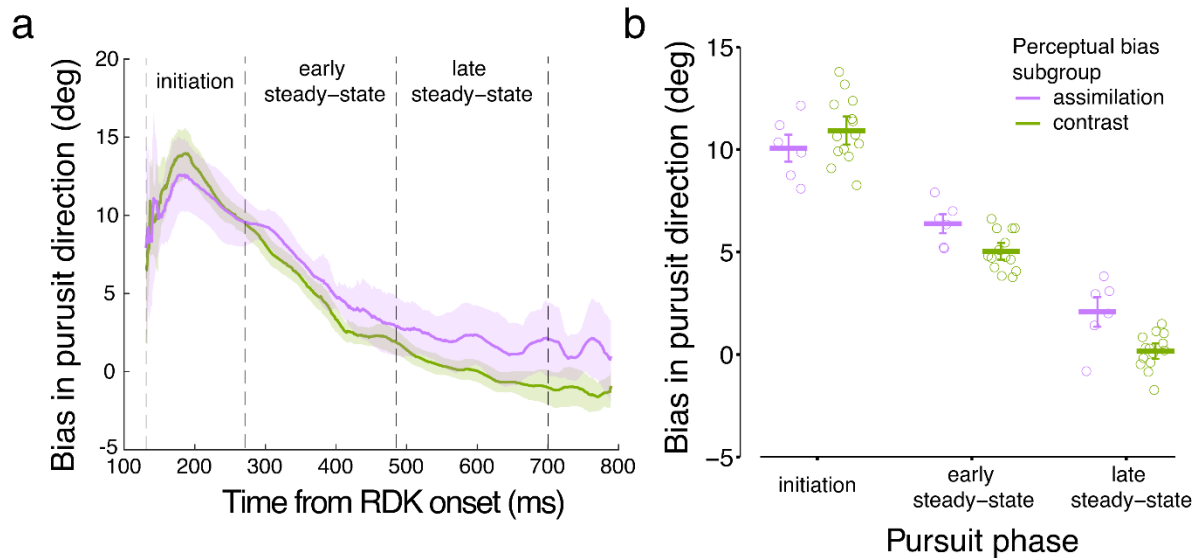
1 **Supporting information: Further exploratory analyses between perceptual** 2 **subgroups**

3 The following materials provide details on the further exploratory analyses conducted:
4 In the exploratory analyses, we showed that observers potentially have different perceptual bias
5 patterns (Fig 8). In addition, perceptual biases correlated with pursuit biases (Fig 7). Because
6 pursuit bias was dynamic and appeared to be stronger during the initial pursuit phase (Fig 5 a and
7 b), we further explored whether observers with assimilation perceptual biases consistently showed
8 a larger pursuit bias than observers with contrast perceptual biases over time. If observers with
9 assimilation perceptual biases showed a larger pursuit bias consistently over time, it might reflect
10 a general response tendency in these observers. By contrast, if the difference in pursuit bias
11 between participants with different perceptual biases was developed during later pursuit phases,
12 there might be a later perceptual modulation on pursuit. In addition, as the direct consequence of
13 eye movements is the change in the retinal image, we also examined how net motion energy of
14 retinal image changed over time, and whether it differed between the perceptual subgroups.

16 **S1. Temporal dynamics of pursuit bias between perceptual subgroups**

17 To explore the temporal dynamics of pursuit bias in observers with different perceptual
18 bias patterns, we calculated the average pursuit direction bias in three time windows (S1 Fig a):
19 the initiation phase (from pursuit onset to 140 ms after pursuit onset), the early steady-state phase
20 (the first half of steady-state phase), and the late steady-state phase (the second half of steady-
21 state). We conducted a two-way rmANOVA of pursuit bias with *subgroup* (assimilation and
22 contrast) and *pursuit phase* (initiation, early steady-state, and late steady-state) as factors. We
23 found that compared to the contrast group, the assimilation group had a slower decrease in pursuit
24 bias over time (S1 Fig b), indicated by a significant *subgroup* \times *pursuit phase* interaction effect
25 [$F(2, 36) = 4.88, p = 0.01, \eta_p^2 = 0.21$]. Post-hoc *t*-tests with Tukey-adjusted *p* values showed that
26 pursuit bias did not differ between the assimilation and contrast groups during the initiation [$t(54)$
27 $= -1.43, p = 0.71, 95\% \text{ CI of difference} = (-2.66, 0.93)$] and early steady-state [$t(54) = 2.22, p =$
28 $0.24, 95\% \text{ CI of difference} = (-0.45, 3.14)$] phases. The assimilation group had a stronger pursuit
29 bias than the contrast group only during the late steady-state phase [$t(54) = 3.15, p = 0.03, 95\% \text{ CI}$

30 of difference = (0.12, 3.70)]. In fact, some observers from the contrast group even showed a
 31 negative pursuit bias during the late steady-state phase (S1 Fig b). Overall, the difference in
 32 pursuit biases between people having different perceptual bias patterns developed over time.
 33



34 **S1 Fig.** Biases in perceptual subgroups over time. (a) Color indicates the perceptual bias
 35 subgroup, see legends in panel (b). Solid lines indicate the mean pursuit bias in each subgroup.
 36 Shaded areas indicate the 95% CI. Dashed vertical lines indicate time points of the pursuit
 37 onset, and the start, middle point, and end of the steady-state phase analysis window. (b) Biases
 38 in pursuit direction in perceptual subgroups across the three pursuit phases. Horizontal bars
 39 indicate the mean across observers. Error bars indicate the 95% CI. Circles indicate the mean of
 40 individual observers.
 41

42

43 **S2. Net motion energy between perceptual subgroups**

44 During eye movements, both retinal and extraretinal signals are required to recover the
 45 actual object motion in the world. As people with different perceptual biases tended to have
 46 various magnitudes of pursuit biases, it would be interesting to see how retinal image motion was
 47 affected. In several studies using RDK stimuli, a small proportion of observers perceived motion
 48 in the opposite direction of the RDK, even when the RDK had 100% motion coherence [1]. The
 49 cause of such individual differences is unclear. One explanation is that even 100%-coherence
 50 RDKs could have motion energy [2] in the opposite direction [1,3]. In the current study, motion
 51 energy of the retinal image may not directly correspond to pursuit direction biases, since the
 52 retinal image motion is affected by both speed and direction of the eyes. Therefore, we calculated

53 the motion energy of retinal images over time, to examine whether motion energy of the stimuli
 54 could be a source of the diverse motion perception. If our stimuli contain motion energy in the
 55 opposite direction of internal motion, a diversity in perception might be encouraged.

56 We calculated the averaged bias in the net motion energy of retinal images for each
 57 observer across time. Specifically, for each trial we first generated the 2D retinal image of the dots
 58 across time. Then, two pairs of spatiotemporal filters were convolved with the retinal image to
 59 calculate the net motion energy over time. We adopted the demo code from Mather [4] and used
 60 the spatiotemporal parameters detailed in a previous study [5]. Specifically, each pair of the
 61 spatiotemporal filter was the sum of different combinations of two spatial and two temporal
 62 filters. Each pair was selective for either the upward or the downward direction. The spatial filters
 63 were even and odd symmetric fourth-order Cauchy functions:

$$64 \quad f_1(x, y) = \cos^4(\alpha) \cos(4\alpha) \exp\left(-\frac{x^2}{2\sigma_g^2}\right)$$

$$65 \quad f_2(x, y) = \cos^4(\alpha) \sin(4\alpha) \exp\left(-\frac{x^2}{2\sigma_g^2}\right)$$

66 where $\alpha = \tan^{-1}(y/\sigma_c)$, $\sigma_c = 0.35^\circ$, and $\sigma_g = 0.05^\circ$. The half width of the spatial filters was 0.7° .

67 Two temporal filters were defined by the following functions:

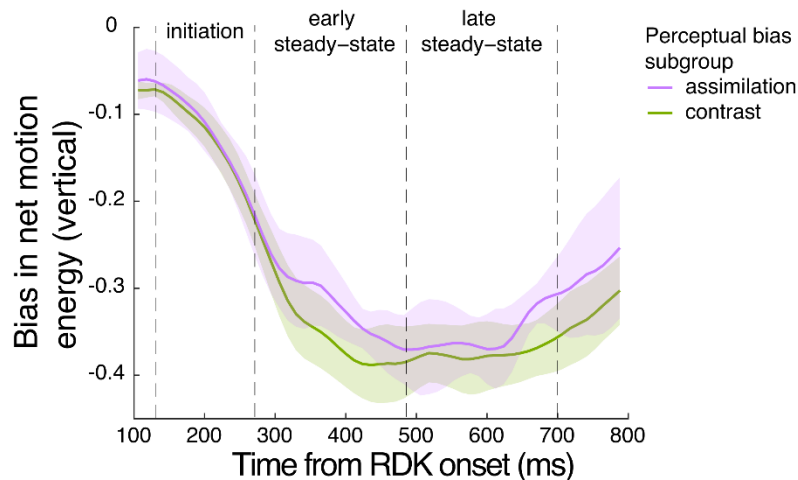
$$68 \quad g_1(t) = (60t)^3 \exp(-60t) \left[\frac{1}{3!} - \frac{(60t)^2}{(3+2)!} \right]$$

$$69 \quad g_2(t) = (60t)^3 \exp(-60t) \left[\frac{1}{5!} - \frac{(60t)^2}{(5+2)!} \right]$$

70 The duration of the temporal filters was chosen to be nine frames, about 106 ms. Since
 71 the pursuit latency was 132 ± 13 ms in the current study, 106 ms was roughly enough time to
 72 gather information for pursuit planning/updating. It was also comparable to the temporal filter
 73 length used in a previous study for pursuit and perception [6]. $f_1g_1 + f_2g_2$ and $f_1g_2 - f_2g_1$
 74 (element-wise multiplication of f and g) would pass information in the upward direction, whereas
 75 $f_1g_2 + f_2g_1$ and $f_1g_1 - f_2g_2$ would pass information in the downward direction. After
 76 convolving each filter with the 3D spatiotemporal retinal image pattern, the results of each pair
 77 were squared and summed up to calculate the motion energy in the upward and downward
 78 direction separately. Then, motion energy in the downward direction was subtracted from that in

79 the upward direction to yield the net motion energy.

80 The net motion energy was normalized between -1 and 1 . A positive bias value indicates
81 more motion energy in the internal motion direction. Surprisingly, we found that our stimuli
82 contained slight motion energy in the opposite direction to internal motion, as shown by the
83 negative bias values during the initial duration before pursuit onset (S2 Fig). With the eyes
84 moving, more motion energy in the opposite direction was observed. The net motion energy of
85 retinal images did not seem to differ between perceptual subgroups, although there seemed to be a
86 trend that the net motion energy of retinal images for the assimilation group is less in the opposite
87 direction to internal motion (S2 Fig).



88
89 **S2 Fig. Biases in net motion energy in the vertical dimension between perceptual**
90 **subgroups.** Positive values indicate that there was more motion energy in the same direction as
91 internal motion. Solid lines indicate the mean of each perceptual subgroup. Shaded areas
92 indicate the 95% CI. Dashed vertical lines indicate time points of the pursuit onset, and the start,
93 middle point, and end of the steady-state phase analysis window.

95 References

- 96 1. Manning C, Meier K, Giaschi D. The reverse motion illusion in random dot motion displays
97 and implications for understanding development. *J Illusion* [Internet]. 2022 Jan 11 [cited
98 2022 Jan 13];3(7916):1–13. Available from:
99 <https://journalofillusion.net/index.php/joi/article/view/7916/14242>
- 100 2. Adelson EH, Bergen JR. Spatiotemporal energy models for the perception of motion. *J Opt*
101 *Soc Am A* [Internet]. 1985 Feb 1 [cited 2022 Jan 13];2(2):284–99. Available from:

- 102 <https://www.osapublishing.org/viewmedia.cfm?uri=josaa-2-2-284&seq=0&html=true>
- 103 3. Bae GY, Luck SJ. Perception of opposite-direction motion in random dot kinematograms.
- 104 Vis cogn [Internet]. 2022 [cited 2022 Apr 13];30(3):1–15. Available from:
- 105 <https://www.tandfonline.com/doi/abs/10.1080/13506285.2022.2052216>
- 106 4. Mather G. Matlab implementation of the Adelson-Bergen motion energy sensor [Internet].
- 107 2013 [cited 2022 Feb 21]. Available from: <http://www.georgemather.com/Model.html>
- 108 5. Kiani R, Hanks TD, Shadlen MN. Bounded integration in parietal cortex underlies decisions
- 109 even when viewing duration is dictated by the environment. J Neurosci [Internet]. 2008 Mar
- 110 19 [cited 2022 Jan 26];28(12):3017–29. Available from:
- 111 <https://www.jneurosci.org/content/28/12/3017>
- 112 6. Mukherjee T, Liu B, Simoncini C, Osborne LC. Spatiotemporal filter for visual motion
- 113 integration from pursuit eye movements in humans and monkeys. J Neurosci. 2017 Feb
- 114 8;37(6):1394–412.